Supplemental Figure Legends

Supplemental Table 1. Peptide identifications for Accurate Mass Tag and Retention Time (AMT) quantitation by mass spectrometry. Proteins identified from our previous proteomics study on quiescent *M. luteus*(1) were used for targeted proteomics analysis by AMT focusing on isocitrate dehydrogenase, isocitrate lyase, malate synthase, and UspA616 (target for knock out). The sequence for each specific peptide (Sequence) for each protein was identified based on parent mass (M/Z (+2))and fragment mass spectra (Spectra given below)and retention times under our chromatographic conditions were tabulated. The average AMT area for Log-phase peak areas (Average Log) and Quiescent-phase (Average Quiescent) were compared and the ratio of Quiescent/Log (Q/Log) was calculated to represent significant changes in protein quantities in these two states. Subsequent mass spectrometry experiments utilized only LC and accurate mass measurements based on human Glu-Fibrinopeptide as an internal standard (*) for both internal mass and retention time calibrations. GroEL (**) was used to confirm protein loading and loss of Hypothetical Protein 359 (***) supported UspA616/UspA712 ratio measurements confirming quiescence. Malate synthase (****) was not resolved in short-gradient (45-minute) LC-MS experiments and required 75-minute gradient experiments for AMT.

Supplemental Figure 1a and 1b. Structure comparison of multiple dual domain Usps. Side and top view of dual domain universal stress proteins from *Escherichia coli* (Blue, 5CB0), *Proteus mirabilis* (Green, 4WY2), *Mycobacterium tuberculosis* (Orange, 3CIS), and *Thermus thermophilus* (Magenta, 3AB7). The internal core structures are essentially identical across these diverse bacterial Usps. Differences observed in the distal helices (right and left side of figures) are due to orientation of the two domains relative to each other in these different structures. Comparison overlays were generated in Chimera (Version 1.12, Build 41623) using the MatchMaker tool. Alignment algorithm was Needleman-Wunsch using BLOSUM-62 matrix and iterative pruning of long atom pairs set to 2.0 angstroms. 3CIS was the reference structure.

Supplemental Figure 2. Multiple sequence alignment using Clustal Omega. Sequences for homologs of UspA616 from *Escherichia coli (UspE/1-316)*, *Proteus mirabilis (PMI_RS05800/1-316)*, *Thermus thermophilus (TTHA0350/1-268)*, *Micrococcus luteus(UspA616/1-324)*, *Pseudomonas aeruginosa (PA4352/1-286)*, *Mycobacterium tuberculosis (Rv2623/1-297)*, and *Mycobacterium smegmatis (MSMEG_3940/1-293)* were aligned using Clustal Omega (https://www.ebi.ac.uk/Tools/msa/) set to default parameters.(2) (**a**) Aspartic acid (D) in the metal binding site is rigorously conserved with a nearby serine (S) retained in most sequences (**Alignment Positions 7-14**). A second metal binding site aspartic acid (D) is conserved in *M. luteus*, *P. aeruginosa*, *M. tuberculosis*, and *M. smegmatis* (lower 4 sequences at **Alignment Position 161**).The first nucleotide binding motif ($GXXG(X)_9G(S/T)$) (Box centered on **Alignment Position 120)** and second nucleotide binding motif (Box centered on **Alignment Position 270-280)** are essentially identical for *M. luteus*, *P. aeruginosa*, *M. tuberculosis*, and *M. smegmatis* with S replaced by N at position 283 in *E. coli* and *P. mirabilis*. However, in this nucleotide binding motif, G_{269} and G_{282} are invariant and presumed to be critical for biological function. Important local structural sidechains rigorously maintained include alanines (A) at Positions 20, 24, 197, a proline-valine motif (PV, Positions 141-142, and glycines (G) at Positions 269 and 282. These invariant residues are likely important for biological function across all compared Usps. (**b**) The phylogenetic tree based on alignment of these sequences (Clustal Omega using BLOSUM62 matrix scores) indicates clusters of similarity between *M. tuberculosis*, *M. smegmatis*, and *M. luteus*. *E. coli* and *P. mirabilis* form their own related cluster. *P. aeruginosa* appears to be more distantly related to Mycobacteria and *T. thermophilus* appears to be primordial in origin.

Supplemental Figure 3. Confirming knockout of *uspA616* gene in *M. luteus* at the genetic and protein level (*ΔuspA616::kan M. luteus*). The uspA616 gene was inactivated by insertion

of a kanamycin resistance cassette. (**Top Left**) Insertion of the kanamycin cassette into the coding sequence of *uspA616* was checked by PCR. The wild-type control identified the smaller *uspA616* coding sequence without insertion (**WT *uspA616*, 1323bp**). The positive control identified the higher molecular weight construct with kanamycin insertion (**Pos. Control, 2587bp**). The knockout *M. luteus* bacterial strain confirmed only the higher molecular weight construct corresponding to the kanamycin insertion (KO Colony). (**Top Right**) Targeted mass spectrometry confirmed inactivation of the *uspA616* gene resulted in loss of UspA616 protein. The Extracted Ion Chromatogram (EIC) for a UspA616-specific peptide (EGVQALLEEVAGK, MH(+2) = 671.8643 amu Monoisotopic Mass) demonstrates this protein was present in the wild-type *M. luteus*, but was below detection limits in the *ΔuspA616 M. luteus* strain. (**Bottom**) Insertion of the *Kan* resistance cassette into the middle of the *uspA616* gene is evidenced by identification of uspA616 sequences both 5' and 3' of the Kan sequence. Whole genome sequencing identified the *Kan* sequence inserted into the uspA616 gene (*uspA616*(197,765-197,622) at the 5' end and *uspA616*(197,591) sequence at the 3' end).

Supplemental Figure 4. High correlation between Accurate Mass tag and Time (AMT) peak area(3) **and Normalized Spectral Abundance Factor (NSAF) quantitation for starvation-regulated proteins.** (**a**) Quantitation data for UspA616, related UspA712, isocitrate lyase, and isocitrate dehydrogenase from AMT data (Supplemental Table 1) and previous NSAF data(1) was compared. Correlation between these different quantitative approaches was excellent, with the obvious limitation of absolute quantitative information as exemplified by UspA616. Because NSAF is a relative quantitative method, the global loss of proteins observed in *M. luteus* quiescence would be reflected as an increase in total abundance for UspA616 (abundance of UspA616 compared to abundance of all other proteins). The AMT data shows UspA616 is retained at constant levels in quiescence when most other proteins exhibit

degradation (for example uspA712). (**b**) The ratio of UspA616 versus UspA712 accurately identified the *M. luteus* quiescent state by AMT and NSAF quantitative measurements. Initial attempts to define quiescence by molecular signature of UspA616 alone were qualitatively successful, but quantitation was limited because of biological variability between samples. We used UspA712 (decreasing in quiescence) combined with UspA616 (retained in quiescence) as an internal control to normalize this variability, providing a successful quantitative signature for quiescence in both NSAF (P=0.0020) and AMT Peak Area (P=0.0031) measurements. All error bars reported are Standard Error of Mean (SEM).

Supplemental Spectra. MS/MS Fragmentation Maps for Peptides Identified in Supplemental Table 1. Peptides in Supplemental Table 1 were identified and confirmed by accurate mass tag/retention time (AMT) and confirmed by fragmentation maps. Each peptide is reported by protein, peptide sequence, accurate mass and charge state, and y-ion (red vertical bar) or b-ion (blue vertical bar) fragments. The y- and b-ions are also labeled on the MS/MS fragmentation spectrum in red for y-ion and blue for b-ion.

Bibliography

1. Mali S, Mitchell M, Havis S, Bodunrin A, Rangel J, Olson G, Widger WR, Bark SJ. 2017. A Proteomic Signature of Dormancy in the Actinobacterium Micrococcus luteus. J Bacteriol 199:e00206-17.

2. Madeira F, Park YM, Lee J, Buso N, Gur T, Madhusoodanan N, Basutkar P, Tivey ARN, Potter SC, Finn RD, Lopez R. 2019. The EMBL-EBI search and sequence analysis tools APIs in 2019. Nucleic Acids Res 47:W636–W641.

3. Stanley JR, Adkins JN, Slysz GW, Monroe ME, Purvine SO, Karpievitch YV, Anderson GA, Smith RD, Dabney AR. 2011. A statistical method for assessing peptide identification confidence in accurate mass and time tag proteomics. Anal Chem 83:6135–6140.

Supplemental Table 1. Peptide identifications for Accurate Mass and Retention Time (AMT) Quantitation by Mass Spectrometry

PROTEIN	PEPTIDE SEQUENCE	M/Z (+2)	ACCURACY	AVERAGE LOG	AVERAGE QUIESCENT	RATIO Q/LOG	RT
Isocitrate Dehydrogenase	AQVLADTLDAATGTLLIEGK	1000.5491	0.01	175936.67	135362.67	0.77	33.70
Isocitrate Dehydrogenase	DYNTDLFPILELGTSAK	948.9831	0.01	323125.56	219310.56	0.68	36.20
Isocitrate Lyase	TDAEAATLITSDVDER	853.9076	0.01	24292.89	667708.67	27.49	25.98
Isocitrate Lyase	LAADVADVPSVIIAR	755.4354	0.01	121499.56	1271853.33	10.47	29.28
Isocitrate Lyase	GEFTNALGALTGNQAVQQVK	1023.5344	0.01	72878.67	667708.67	9.16	30.49
Malate Synthase****	QAEILTDEALAFLGR	823.9410	0.01	487541.50	123273.49	0.25	34.50
Universal Stress Protein A 616	EGVQALLEEVAGK	671.8643	0.01	309019.22	317780.00	1.03	32.64
GroEL*	EVELEDPYENMGAQLAK	968.4539	0.01	1615188.67	711681.33	0.44	28.54
GroEL*	LEQADLDVLGSAR	693.8648	0.01	1384177.89	1403111.67	1.01	26.86
Glu-Fibrinopeptide**	EGVNDNEEGFFSAR	785.8421	0.01	3800714.33	5268191.78	1.39	25.98
Hypothetical Protein 359***	TAMEAVYQLLDVER	819.4138	0.01	636230.22	38412.00	0.06	34.95

Supplemental Figure 1A

Supplemental Figure 1B

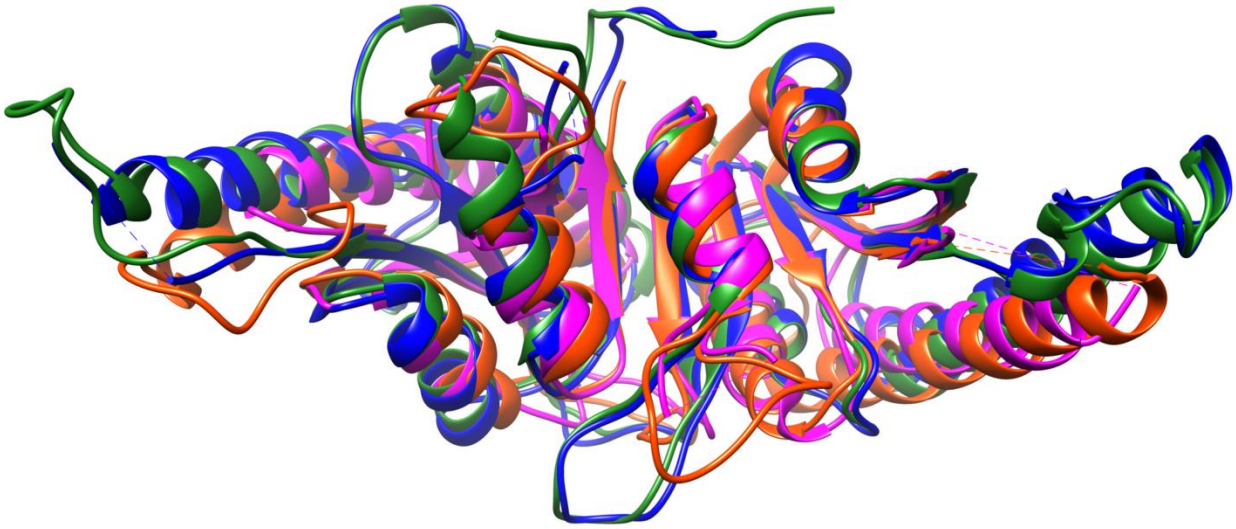

Supplemental Figure 2A

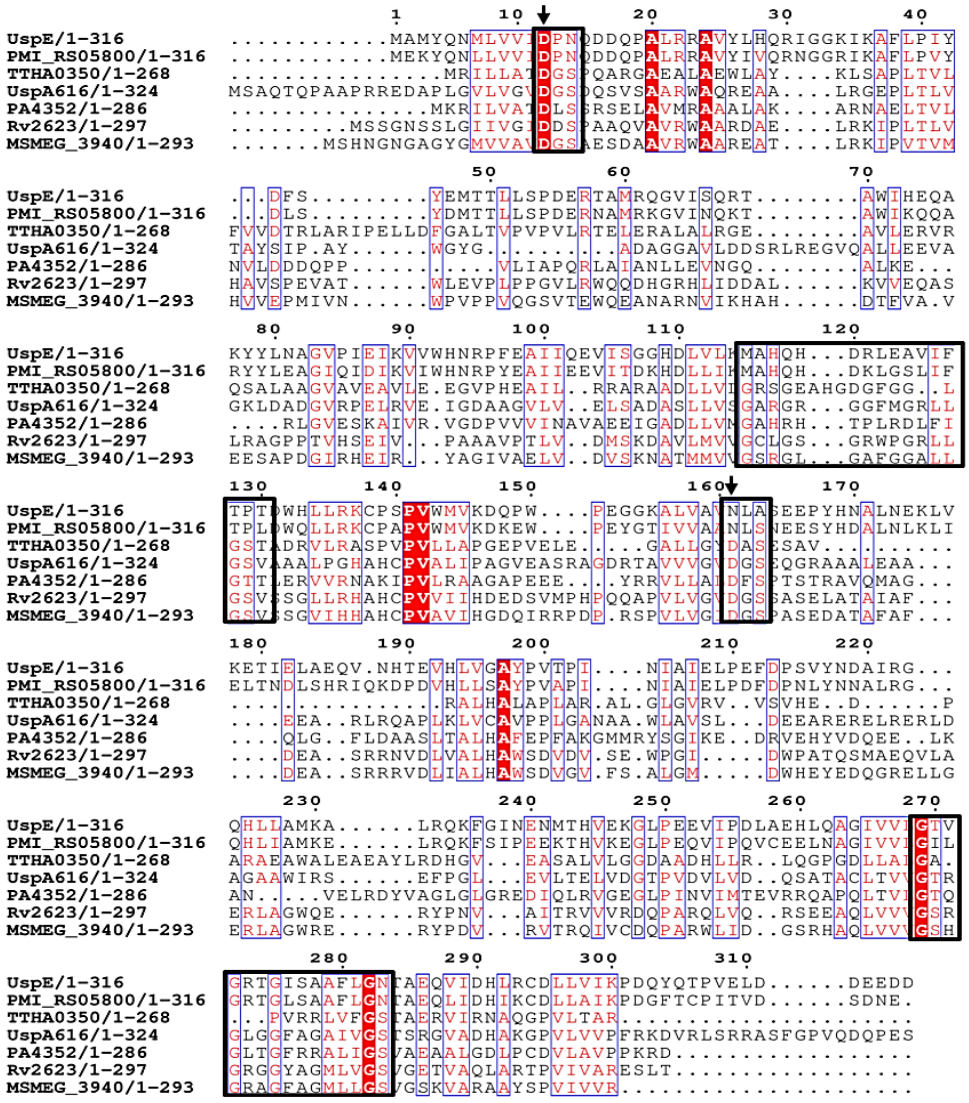

Supplemental Figure 2B

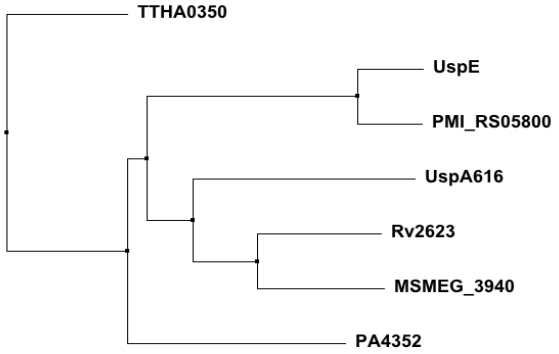

Supplemental Figure 3

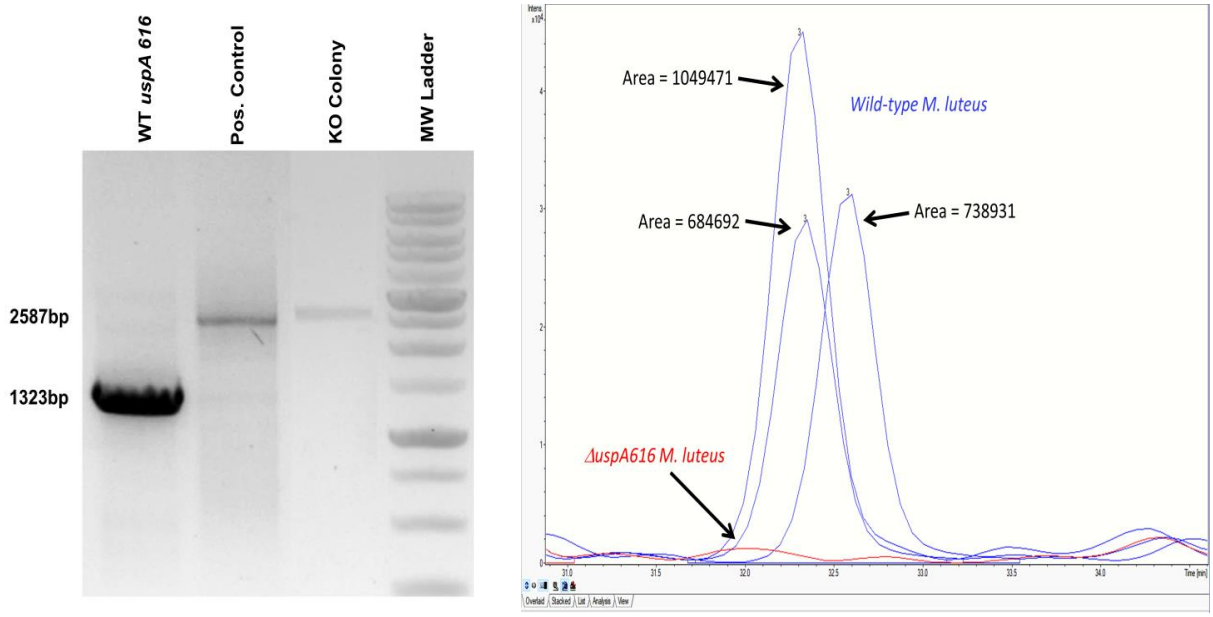

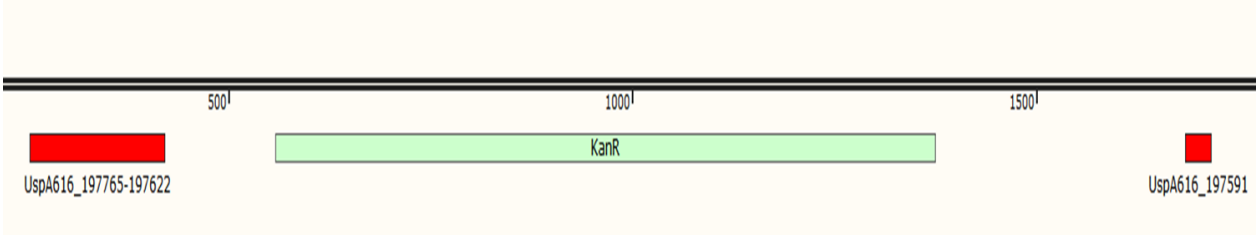

CCGCGACGCCGCGGCTCGTGGAGCCGACGATCGCACCGGCGAAGCCGCCCAGGCCGCGCGTGCCCACCAC
GGTGAGGCAGGCGGTGGCGCTCTGGTCCACCAACACGTCCACGGGGGTGCCGTCCACGAGCTCGGTGAGGA
CCTCGAGGCCGGGGAACTCGGAGCGGATCCGTCGACCTGCAGGGGGGGGGGGGAAAGCCACGTTGTGTCTC
AAAATCTCTGATGTTACATTGCACAAGATAAAAATATATCATCATGAACAATAAAACTGTCTGCTTACATAAACAGT
AATACAAGGGGTGTT**ATGAGCCATATTCAACGGGAAACGTCTTGCTCGAGGCCGCGATTAAATTCCAACATGG**
ATGCTGATTTATATGGGTATAAATGGGCTCGCGATAATGTCGGGCAATCAGGTGCGACAATCTATCGATTGTAT
GGGAAGCCCGATGCGCCAGAGTTGTTTCTGAAACATGGCAAAGGTAGCGTTGCCAATGATGTTACAGATGAG
ATGGTCAGACTAAACTGGCTGACGGAATTTATGCCTCTTCCGACCATCAAGCATTTTATCCGTACTCCTGATGA
TGCATGGTTACTCACCACTGCGATCCCCGGGAAAACAGCATTCCAGGTATTAGAAGAATATCCTGATTCAGGT
GAAAATATTGTTGATGCGCTGGCAGTGTTCCTGCGCCGGTTGCATTCGATTCCTGTTTGTAATTGTCCTTTTAAC
AGCGATCGCGTATTTCGTCTCGCTCAGGCGCAATCACGAATGAATAACGGTTTGGTTGATGCGAGTGATTTTG
ATGACGAGCGTAATGGCTGGCCTGTTGAACAAGTCTGGAAAGAAATGCATAAGCTTTTGCCATTCTCACCGGA
TTCAGTCGTCACTCATGGTGATTTCTCACTTGATAACCTTATTTTTGACGAGGGGAAATTAATAGGTTGTATTGA
TGTTGGACGAGTCGGAATCGCAGACCGATACCAGGATCTTGCCATCCTATGGAACTGCCTCGGTGAGTTTTCT
CCTTCATTACAGAAACGGCTTTTTCAAAAATATGGTATTGATAATCCTGATATGAATAAATTGCAGTTTCATTTG
ATGCTCGATGAGTTTTTCTAATCAGAATTGGTTAATTGGTTGTAACACTGGCAGAGCATTACGCTGACTTGACGG
GACGGCGGCTTTGTTGAATAAATCGAACTTTTGCTGAGTTGAAGGATCAGATCACGCATCTTCCCGACAACGCA
GACCGTTCCGTGGCAAAGCAAAAGTTCAAAATCACCAACTGGTCCACCTACAACAAAGCTCTCATCAACCGTGG
CTCCCTCACTTTCTGGCTGGATGATGGGGCGATTCAGGCCTGGTATGAGTCAGCAACACCTTCTTCACGAGGCA
GACCTCAGCGCCCCCCCCCCCCTGCAGGTCGACG**GATCCACGCGGCGCCGGCGTCGAGACGCTCG**

Supplemental Figure 4A

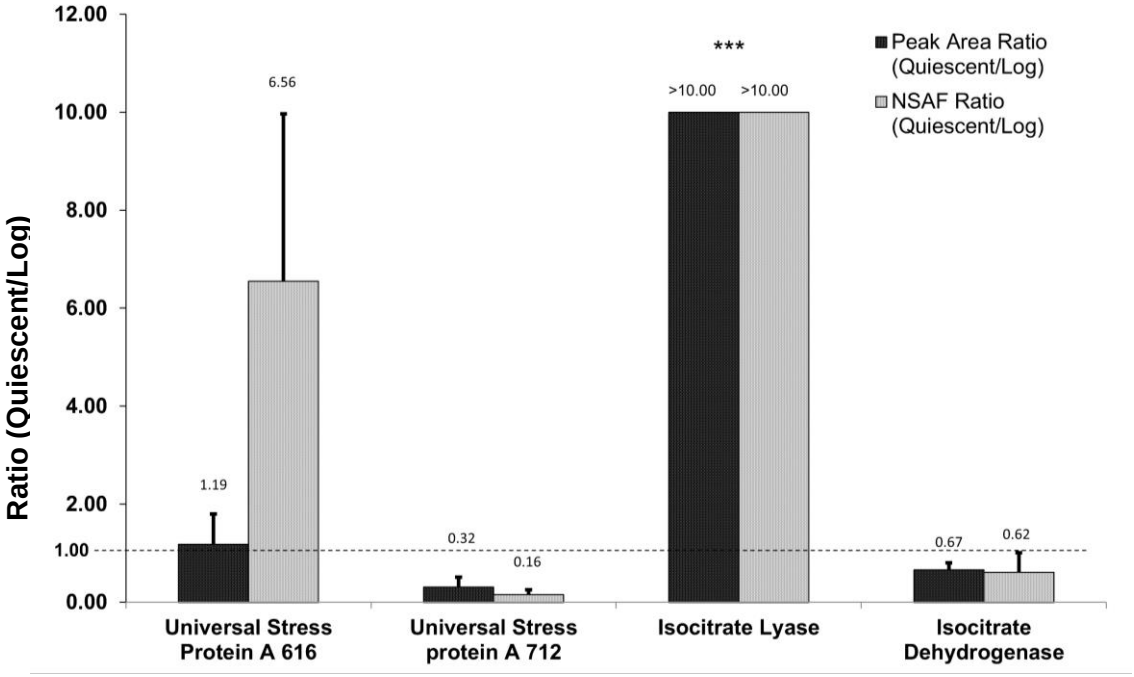

Supplemental Figure 4B

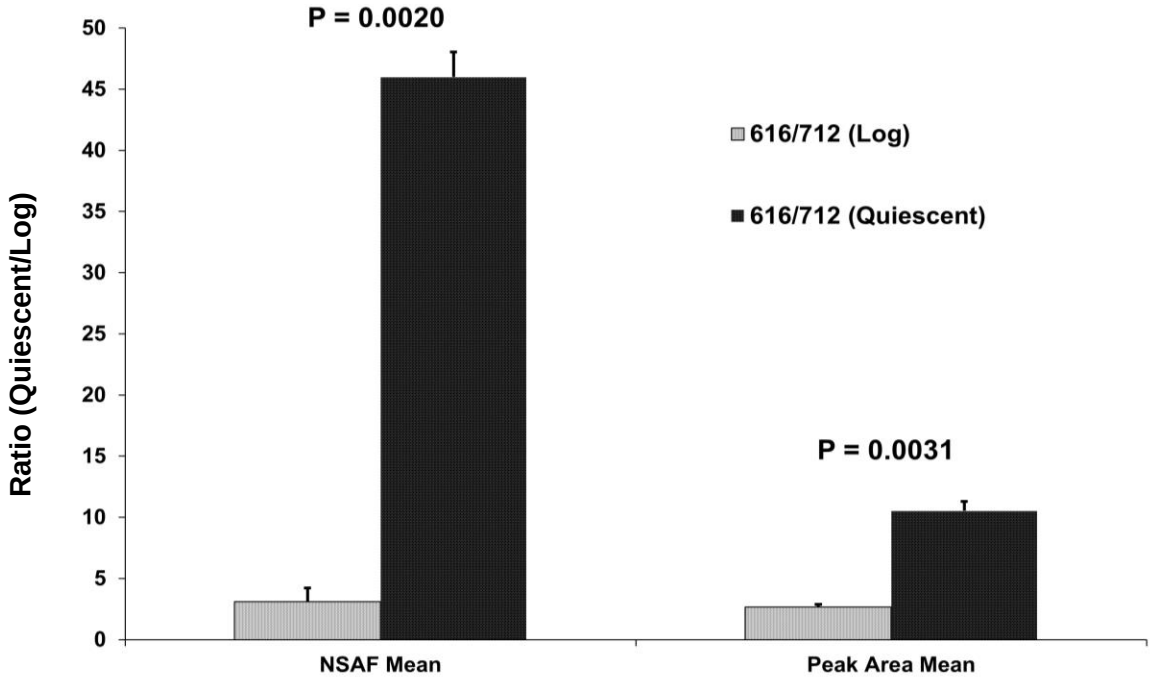

Supplemental Spectra

GroEL EVELEDPYENMGAQLAK 968.4539 (+2)

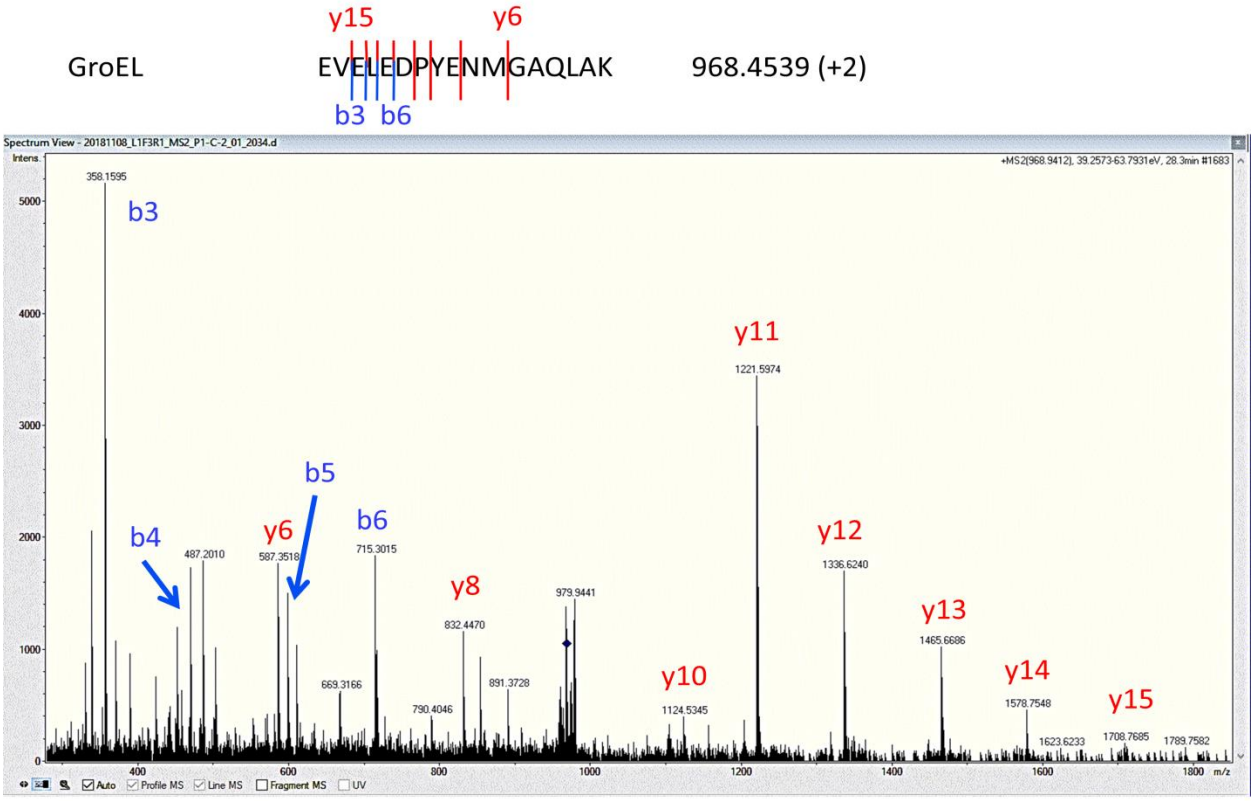

GroEL LEQADLDVLGSAR 693.8648 (+2)

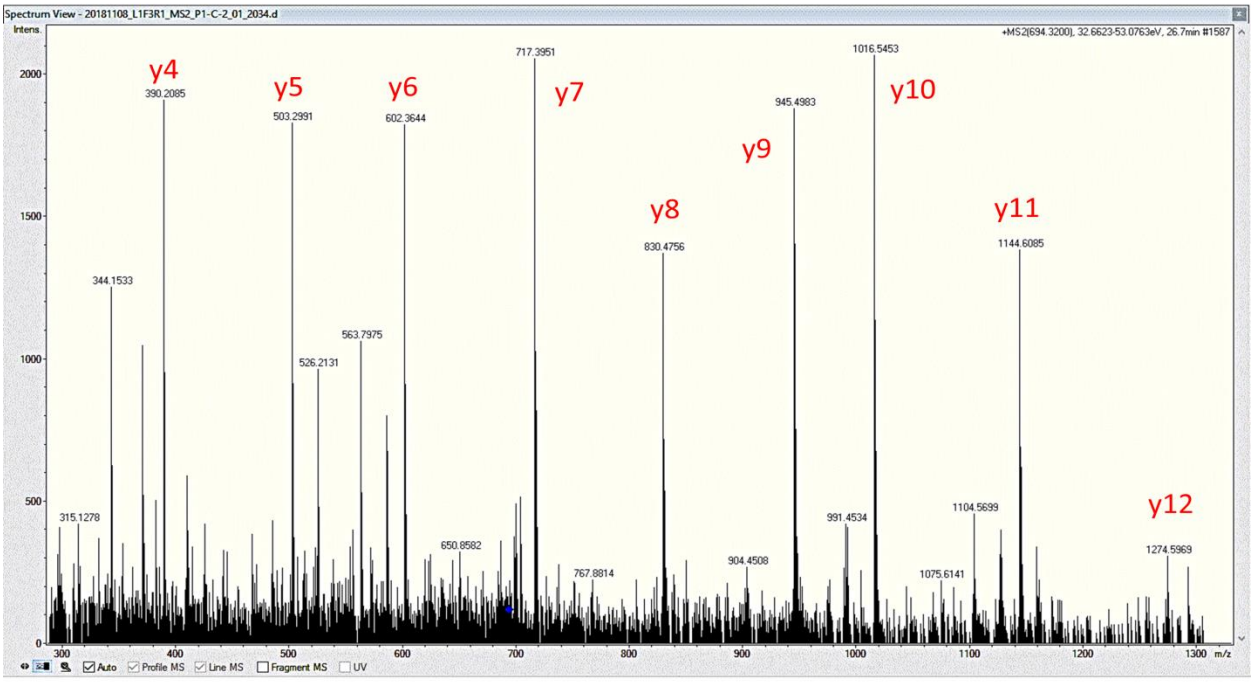

Isocitrate Dehydrogenase AQVLADTLDAATGTLLIEGK 1000.5491 (+2)

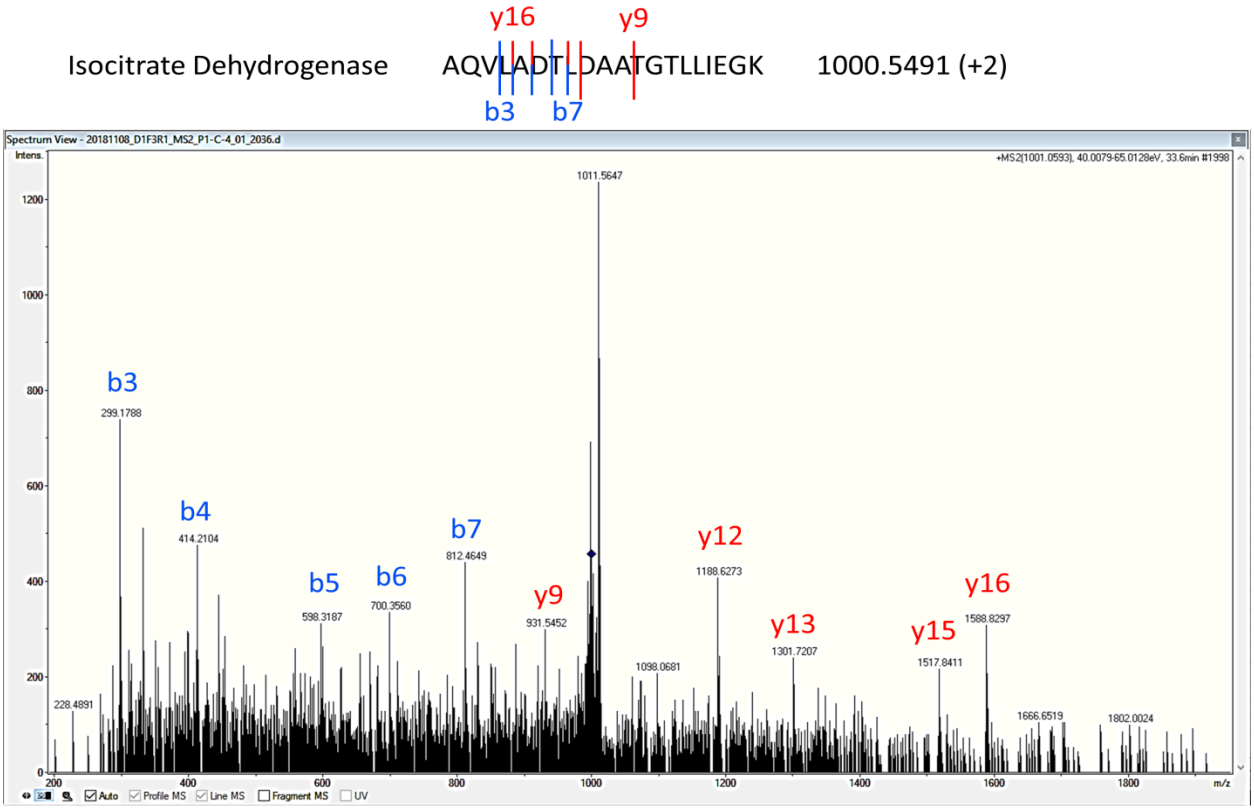

Isocitrate Dehydrogenase DYNTDLFPILELGTSAK 948.9831 (+2)

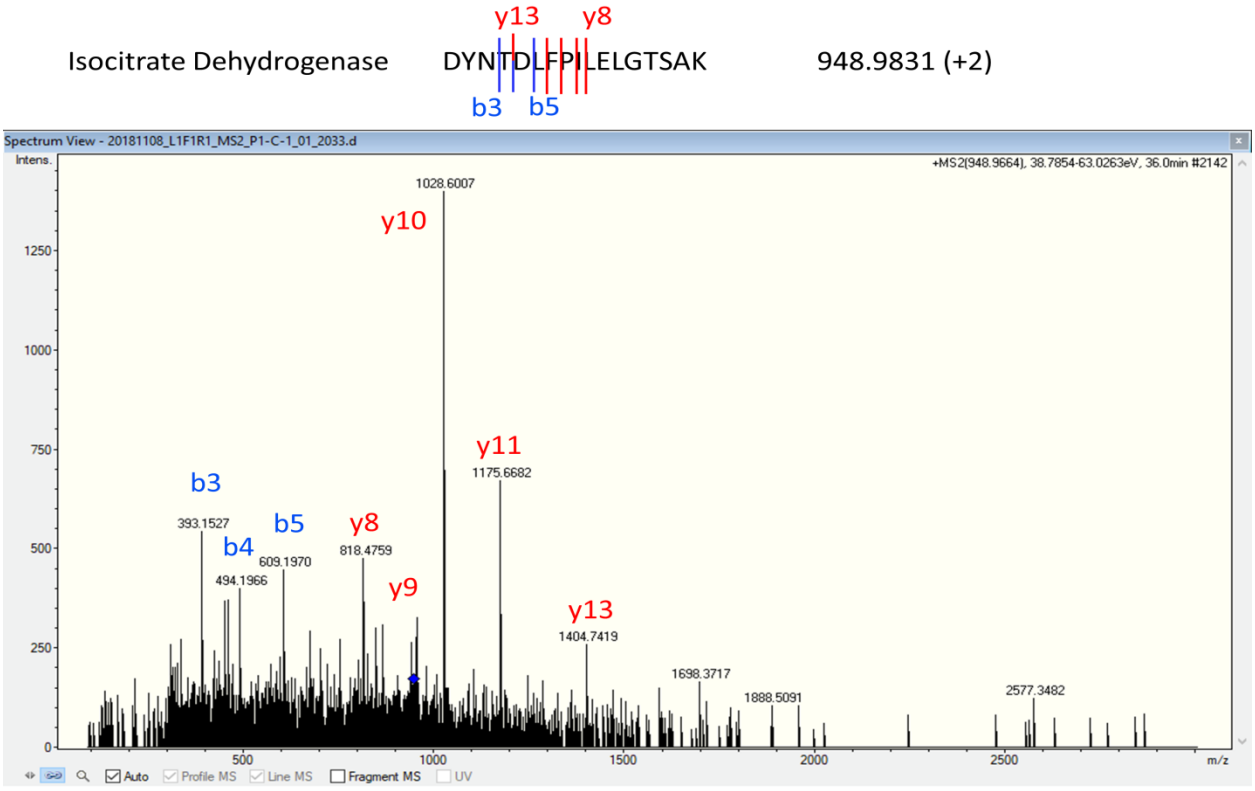

Isocitrate Lyase TDAEAATLITSDVDER 853.9076 (+2)

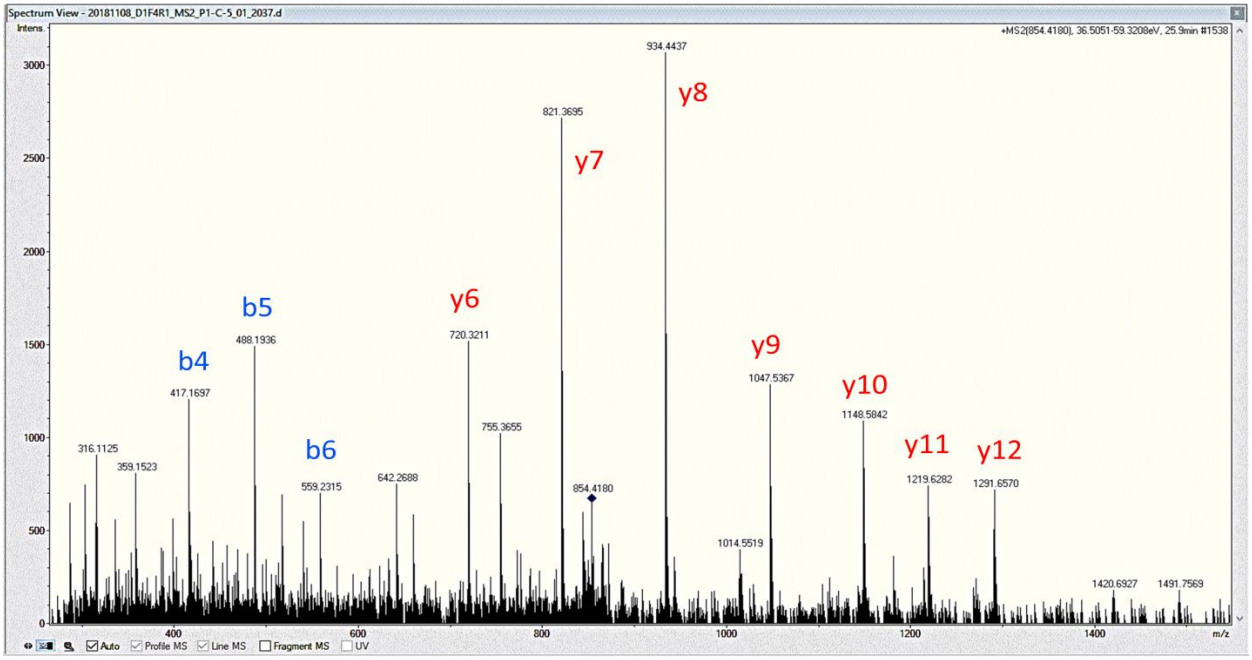

Isocitrate Lyase LAADVADVPSVIIAR 755.4354 (+2)

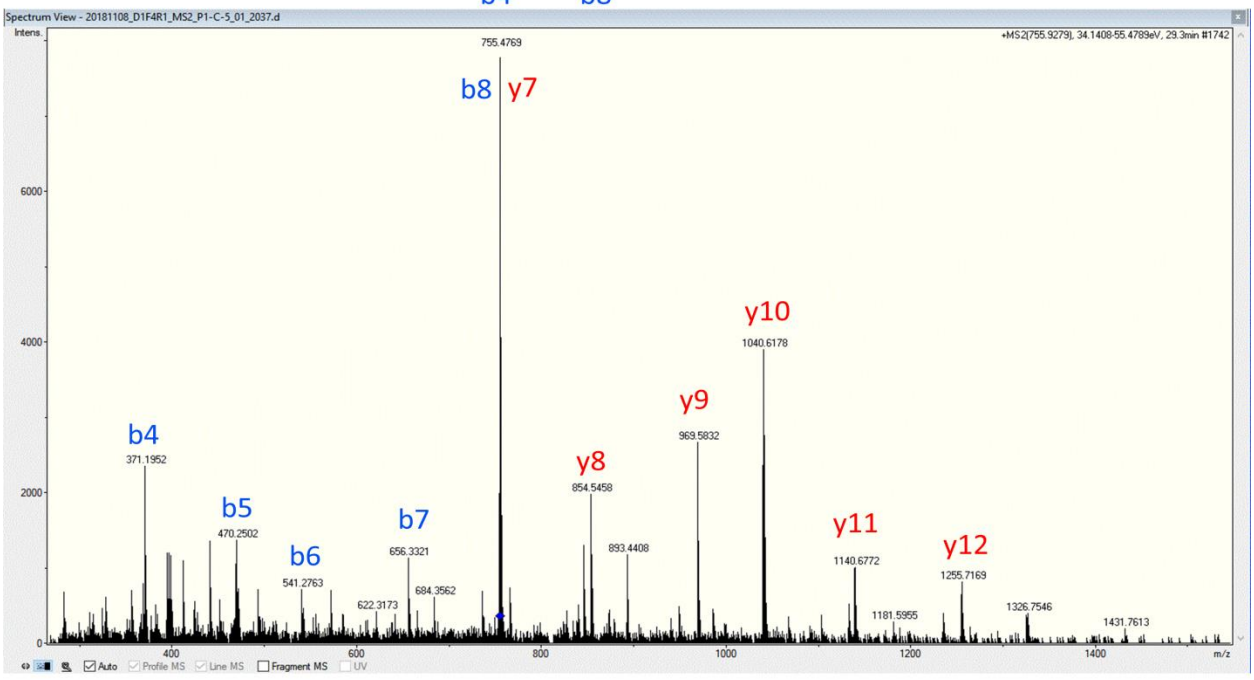

Isocitrate Lyase GEFTNALGALTGNQAVQQVK 1023.5344 (+2)

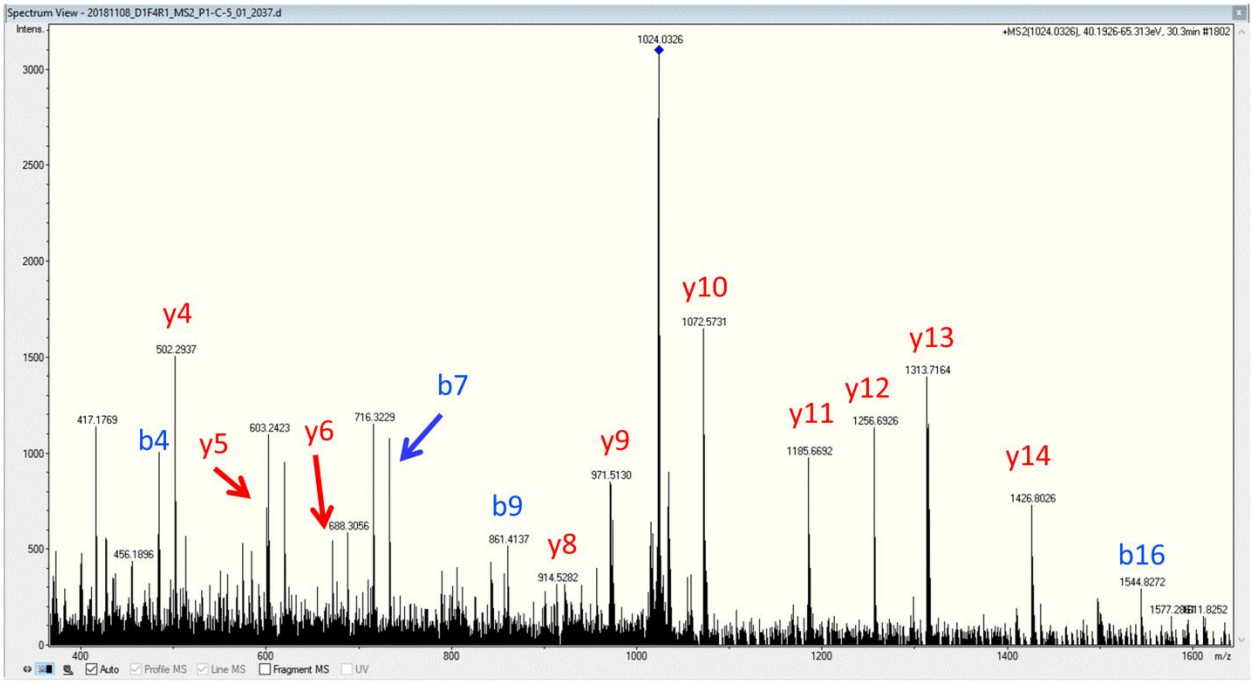

Universal Stress Protein 616 EGVQALLEEVAGK 671.8643 (+2)

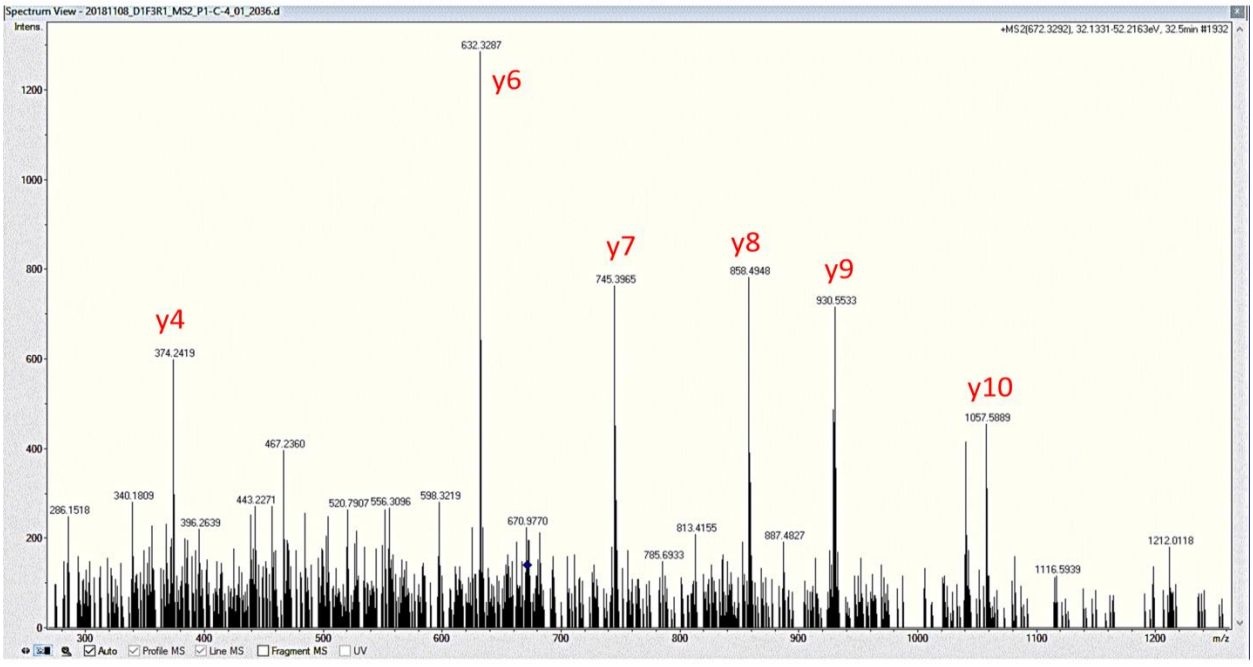

Hypothetical Protein 359 TAMEAVYQLLDVER 819.4138 (+2)